

The Levermore-Pomraning and Atomic Mix Closures for n-ary Stochastic Materials

Shawn D. Pautz and Brian C. Franke

Sandia National Laboratories: Albuquerque, NM, 87185-1179, {sdpautz,bcfrank}@sandia.gov

Abstract – We examine radiation transport in stochastic media consisting of an arbitrary number of materials. We derive the statistical transport equations and LP closure for such media when the material statistics is Markovian. The atomic mix closure, previously derived in one-dimensional slab geometry for binary media, is extended to an arbitrary number of materials. Results demonstrate that the atomic mix closure is generally more accurate than the LP closure, but is problematic for higher-order quadratures when the problem is sufficiently thick. In such cases a subgrid model may be used, which is also observed to be more accurate than the LP model.

I. INTRODUCTION

Much of the past research into the accurate modeling of stochastic media in radiation transport calculations has focused on binary media. A few early papers performed some theoretical analysis with an arbitrary number of materials [1,2], but extension and application appear to be limited to binary media. In the present work we extend some of this analysis to an arbitrary number of materials. We derive generalizations of the statistical transport equation and the Levermore-Pomraning (LP) closure [1,3,4] for such problems when the material statistics is Markovian. We also generalize the atomic mix closure [5], which we observe to be more accurate than LP in almost all cases studied.

Our work is organized as follows. In Section II we derive various equations and closures for an arbitrary number of materials. In Section III we present results for these models and compare them against benchmarks. We present conclusions and suggestions for future work in Section IV.

II. DESCRIPTION OF THE ACTUAL WORK

1. Extension of Statistical Transport Equation and LP Closure

In [1] is a formal derivation of the energy-dependent statistical transport equation for arbitrary mixing statistics and also a derivation of what is now generally called the LP closure. At about the same time a different derivation of the monoenergetic statistical transport equation and corresponding LP closure based on a control volume approach was obtained for binary media [4]. In this section we extend the latter analysis to an arbitrary number of materials for Markovian media.

In [4] the following balance equation was derived:

$$\frac{1}{v} \frac{\partial [p_i \langle \psi_i \rangle]}{\partial t} + \vec{\Omega} \cdot \nabla [p_i \langle \psi_i \rangle] + \sigma_{t,i} p_i \langle \psi_i \rangle = \frac{\sigma_{s,i}}{4\pi} p_i \int d\vec{\Omega}' \langle \psi_i(\vec{\Omega}') \rangle + p_i q_i + \theta_i \quad (1a)$$

$$\theta_i = - \lim_{V \rightarrow 0} \left[\frac{1}{V} \langle \psi(\vec{\Omega}) \int_{\Gamma} ds \vec{n}_i \cdot \vec{\Omega} \rangle \right] \quad (1b)$$

Here θ_i describes the average fluxes crossing a material interface into or out of material i . Although subsequent analysis was restricted to binary media, Eqs. (1) are actually valid for an arbitrary number of materials.

In a manner more general than that in [4] we can rewrite θ_i in terms of specific types and orientations of interfaces:

$$\theta_i = \lim_{V \rightarrow 0} \frac{1}{V} \left[- \sum_{j \neq i} \langle \psi(\vec{\Omega}) \int_{\Gamma_{ij}} ds \vec{n}_i \cdot \vec{\Omega} \rangle + \sum_{j \neq i} \langle \psi(\vec{\Omega}) \int_{\Gamma_{ji}} ds \vec{n}_j \cdot \vec{\Omega} \rangle \right] \quad (2)$$

We can rewrite Eq. (2) as:

$$\theta_i = - \sum_{j \neq i} \langle \psi_{s,ij} \rangle Q_{ij}(\vec{\Omega}) + \sum_{j \neq i} \langle \psi_{s,ji} \rangle Q_{ji}(\vec{\Omega}) \quad (3a)$$

$$\langle \psi_{s,ij} \rangle = \langle \psi(\vec{\Omega}) \int_{\Gamma_{ij}} ds \vec{n}_i \cdot \vec{\Omega} \rangle / \langle \int_{\Gamma_{ij}} ds \vec{n}_i \cdot \vec{\Omega} \rangle \quad (3b)$$

$$Q_{ij}(\vec{\Omega}) = \lim_{V \rightarrow 0} \left[\frac{1}{V} \langle \int_{\Gamma_{ij}} ds \vec{n}_i \cdot \vec{\Omega} \rangle \right] \quad (3c)$$

By means of a differential volume analysis we obtain:

$$Q_{ij}(\vec{\Omega}) = \frac{p_i}{\lambda_i} P(j|i) \quad (4)$$

The physical interpretation of Eq. (4) is that p_i is the probability that an arbitrary location is in material i , λ_i is the probability per unit path length that there is an interface there, and $P(j|i)$ is the probability that material j is on the other side of the interface. A similar result was obtained in [4], where $P(j|i)$ was identically unity since only binary media were

considered. In the present analysis for an arbitrary number of materials $P(j|i)$ depends on the material statistics.

For the sake of our analysis we assume that we are dealing with Markovian media. In that case we can use the following expressions:

$$P(j|i) = \frac{p_j}{1-p_i} \quad (5a)$$

$$\lambda_c = \lambda_i(1 - p_i), \forall i \quad (5b)$$

Combining the above equations gives a monoenergetic statistical transport equation for Markovian media with an arbitrary number of materials:

$$\begin{aligned} \frac{1}{v} \frac{\partial [p_i \langle \psi_i \rangle]}{\partial t} + \vec{\Omega} \cdot \nabla [p_i \langle \psi_i \rangle] + \sigma_{t,i} p_i \langle \psi_i \rangle \\ = \frac{\sigma_{s,i}}{4\pi} p_i \int d\vec{\Omega}' \langle \psi_i(\vec{\Omega}') \rangle + p_i q_i \\ + \lambda_c^{-1} p_i \sum_{j \neq i} p_j [\langle \psi_{s,ji} \rangle - \langle \psi_{s,ij} \rangle] \end{aligned} \quad (6)$$

If we assume stationary statistics, we obtain:

$$\begin{aligned} \frac{1}{v} \frac{\partial \langle \psi_i \rangle}{\partial t} + \vec{\Omega} \cdot \nabla \langle \psi_i \rangle + \sigma_{t,i} \langle \psi_i \rangle \\ = \frac{\sigma_{s,i}}{4\pi} \int d\vec{\Omega}' \langle \psi_i(\vec{\Omega}') \rangle + q_i \\ + \lambda_c^{-1} \sum_{j \neq i} p_j [\langle \psi_{s,ji} \rangle - \langle \psi_{s,ij} \rangle] \end{aligned} \quad (7)$$

This equation is formally exact for stationary Markovian mixing statistics. Unfortunately, an additional set of equations is needed to relate the two types of conditional averages. The LP closure, generalized to an arbitrary number of materials, is obtained by assuming that $\langle \psi_{s,ij} \rangle = \langle \psi_i \rangle$:

$$\begin{aligned} \frac{1}{v} \frac{\partial \langle \psi_i \rangle}{\partial t} + \vec{\Omega} \cdot \nabla \langle \psi_i \rangle + \sigma_{t,i} \langle \psi_i \rangle \\ = \frac{\sigma_{s,i}}{4\pi} \int d\vec{\Omega}' \langle \psi_i(\vec{\Omega}') \rangle + q_i \\ + \lambda_c^{-1} \sum_{j \neq i} p_j (\langle \psi_j \rangle - \langle \psi_i \rangle) \end{aligned} \quad (8)$$

For binary materials Eqs. (7) and (8) reduce to their more familiar forms.

2. Derivation of Atomic Mix Closure

In [5] we derived a new ‘‘atomic mix’’ closure for binary stochastic media. Here we repeat that derivation for an arbitrary number of materials.

In [6] we proposed a family of closures of the following form:

$$[\langle \psi_s \rangle] = R[\langle \psi \rangle] \quad (9)$$

To determine R we proposed a set of subsidiary calculations to relate $[\langle \psi_s \rangle]$ and $[\langle \psi \rangle]$ to boundary fluxes $[\langle \psi_b \rangle]$:

$$\begin{aligned} [\langle \psi \rangle] &= R_u[\langle \psi_b \rangle], \\ [\langle \psi_s \rangle] &= R_s[\langle \psi_b \rangle] = R_s R_u^{-1}[\langle \psi \rangle] \equiv R[\langle \psi \rangle] \end{aligned} \quad (10)$$

These subsidiary calculations involve a deterministically-generated ensemble of geometric realizations; weighted transport calculations on this ensemble yield numerical approximations to R . Depending on the problem this ensemble can be quite large. We note that the LP closure uses the identity matrix for R in Equation (9).

In order to develop our new model for R we depict an arbitrary realization in Figure 1 for a stochastic transport problem in one-dimensional slab geometry. In the regions centered around location r we explicitly note the distinct materials at the extremities and on either side of r ; there may be material interfaces within these regions (not depicted). These are surrounded by ‘‘buffer’’ regions extending to the problem boundary in which we replace distinct material regions with atomically mixed material. The motivation for the atomic mix layers is to reduce the number of explicit material regions and interfaces that we will eventually need to computationally model; we assume that material distribution details near r are more important. We depict the (known) boundary fluxes and the (unknown) fluxes at r . This is a generalization of the approach we took in [6], which did not include any atomic mix layers and was specialized for the ‘‘rod’’ (two-point Gauss-Lobatto angular quadrature) problem.

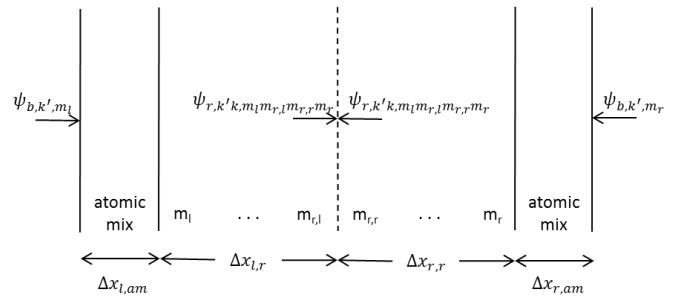


Fig. 1. General slab-geometry stochastic transport model.

With the above description of the problem we can relate the conditionally-averaged interior fluxes to the boundary fluxes as a function of the material distributions:

$$\begin{aligned} \langle \psi_{k,m_r^-} \rangle &= p_{m_r^-}^{-1} \sum_{k'} \sum_{m_r^+} \sum_{m^-} \sum_{m^+} p_{r,m_r^- m_r^+ m^- m^+} R_{r,k',k,m_r^- m_r^+ m^- m^+} \psi_{b,k',m^-} \\ \langle \psi_{s,k,m_r^-} \rangle &= p_{m_r^-}^{-1} \sum_{k'} \sum_{m_r^+ \neq m_r^-} \sum_{m^-} \sum_{m^+} p_{r,m_r^- m_r^+ m^- m^+} R_{s,r,k',k,m_r^- m_r^+ m^- m^+} \psi_{b,k',m^-} \end{aligned} \quad (11)$$

The various response functions R in Equation (11) are derived from ensemble-averages of the conditional interior fluxes depicted in Figure 1 and are in general unknown.

In [6] Equation (11) was approximately solved by creating a finite ensemble of realizations, performing transport calculations on each realization for each boundary flux, and then using the computed interior fluxes to obtain R . We had intended (and still do intend) to perform a similar process in the present work, which we hope will obtain reasonable accuracy at reduced computational cost. However, we have discovered an interesting limit which has proved quite fruitful and forms the basis of the atomic mix closure.

If we allow $\Delta x_{l,r} \rightarrow \Delta x_{r,r} \rightarrow 0$ and the atomic mix buffer regions to grow accordingly, we find that $m_l \rightarrow m_{r,l}$ and $m_r \rightarrow m_{r,r}$. In this limit we find that Equation (11) simplifies to

$$\begin{aligned} \langle \psi_{k,m_r^-} \rangle &= \sum_{k'} R_{r,k',k} \psi_{b,k',m_r^-} \\ \langle \psi_{s,k,m_r^-} \rangle &= \begin{cases} \sum_{\mu_{k'} > 0} R_{r,k',k} \psi_{b,k',m_r^-} + \sum_{\mu_{k'} < 0} R_{r,k',k} \sum_{m_r^+ \neq m_r^-} \frac{p_{m_r^+}}{1 - p_{m_r^-}} \psi_{b,k',m_r^+}, \mu_k > 0 \\ \sum_{\mu_{k'} > 0} R_{r,k',k} \sum_{m_r^+ \neq m_r^-} \frac{p_{m_r^+}}{1 - p_{m_r^-}} \psi_{b,k',m_r^+} + \sum_{\mu_{k'} < 0} R_{r,k',k} \psi_{b,k',m_r^-}, \mu_k < 0 \end{cases} \end{aligned} \quad (12)$$

where the first equation defines the elements of R_u and the second one defines R_s . We note two important properties of this equation. First, R_u and R_s contain similar matrix elements but with various permutations and weighted sums. This results directly from the fact that in this thin limit there are either no material interfaces (with probability approaching unity) or there is a single material interface (with probability approaching unity, conditioned on there being at least one interface). If there are no material interfaces the driving boundary flux will traverse the same material both upstream and downstream of the location of interest. If there is a material interface the driving flux will pass through the material of interest and then some other material (or vice versa). Interestingly, if we do not make this distinction then $R_u = R_s$ and we obtain the LP closure. Second, each $R_{r,k',k}$ can be obtained by transport calculations on a *single* realization, namely one filled entirely with atomically mixed materials. This can be accomplished with N transport calculations, where N is the number of angular quadrature points, for R at some location in the domain (R in general is spatially dependent). If the angular quadrature is symmetric one may use only $N/2$ calculations.

III. RESULTS

In order to test the above models, we reexamine the benchmark problems first reported in [4]. These problems consist of nine different combinations of binary media and mixing statistics for three different slab widths. The material properties of these tests are listed in Table I, where we note that cases 1 and 4, 2 and 5, and 3 and 6, respectively, differ only in their characteristic chord lengths (in subsequent discussion any reference to cases 1, 2, or 3 will implicitly include cases 4, 5, and 6). The problems are monoenergetic in one-dimensional slab geometry; both the rod and ‘‘planar’’ (S_{16} Gauss-Legendre) variants are studied. The problems are driven by an isotropic flux on the left boundary. All scattering is isotropic. The reflected and transmitted currents are the transport quantities examined. In the present work we do not restrict ourselves to the particular chord lengths in Table I; instead we examine a continuum of length scales. We also do not restrict ourselves to binary media; we freely form additional combinations of those materials.

Table I. Stochastic material properties [4]

case	$\sigma_{t,0}$	$\sigma_{t,1}$	c_0	c_1	λ_0	λ_1
1	10/99	100/11	0	1	99/100	11/100
2	10/99	100/11	1	0	99/100	11/100
3	10/99	100/11	0.9	0.9	99/100	11/100
4	10/99	100/11	0	1	99/10	11/10
5	10/99	100/11	1	0	99/10	11/10
6	10/99	100/11	0.9	0.9	99/10	11/10
7	2/101	200/101	0	1	101/20	101/20
8	2/101	200/101	1	0	101/20	101/20
9	2/101	200/101	0.9	0.9	101/20	101/20

We generated the atomic mix results and atomic mix response matrices in Equation (12) with the Sceptre deterministic code [7] using its discretization of the first-order form of the linear monoenergetic Boltzmann equation. Unaccelerated source iteration errors were controlled to be less than 10^{-7} with the aid of spectral radius estimates to guard against false convergence. Uniform mesh refinement and Richardson extrapolation were used to achieve a spatial error of less than 10^{-6} . A variant of Sceptre that can solve Equations (8) and (9) was used to obtain LP and atomic mix closure results. We also used Sceptre to generate benchmarks using Monte Carlo sampling to create ensembles of realizations. Each realization was solved with iterative errors below 10^{-4} and spatial errors below 10^{-3} ; sufficient realizations were used to obtain statistical errors less than 1% in most cases.

1. Rod Problems

A few of our results for the rod problems are presented in Figures 2-7 for a slab thickness $\Delta x=1$ and in Figures 8-13 for $\Delta x=10$. These figures depict the reflected and transmitted

fluxes in one binary material (the continuum involving case 1), in four materials (equal proportions of cases 1 and 2), and in twelve materials (equal proportions of all unique materials listed in Table I). These figures contain results for our benchmark calculations, for an atomic mix calculation, for the LP treatment, and for the atomic mix closure (using the response matrix computed in the center of the geometry). Note that the “atomic mix” results are the directly computed reflection and transmission from an atomic mix realization, not the results generated by means of the corresponding closure.

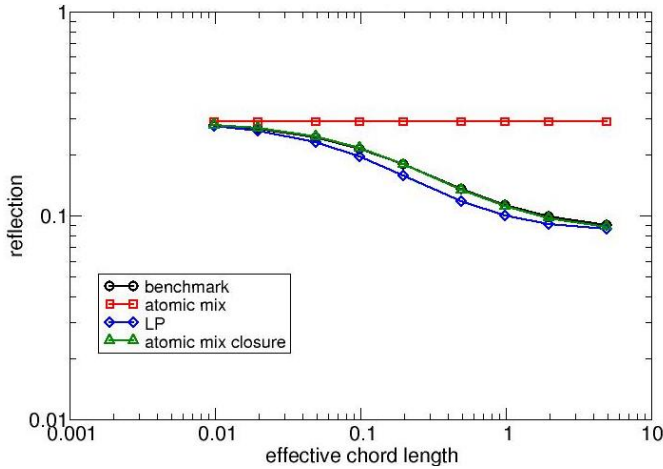


Fig. 2. Reflection results, case 1, rod, $\Delta x=1$.

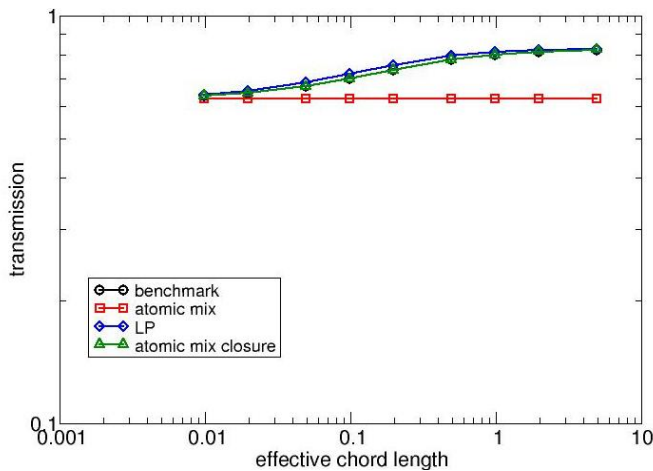


Fig. 3. Transmission results, case 1, rod, $\Delta x=1$.

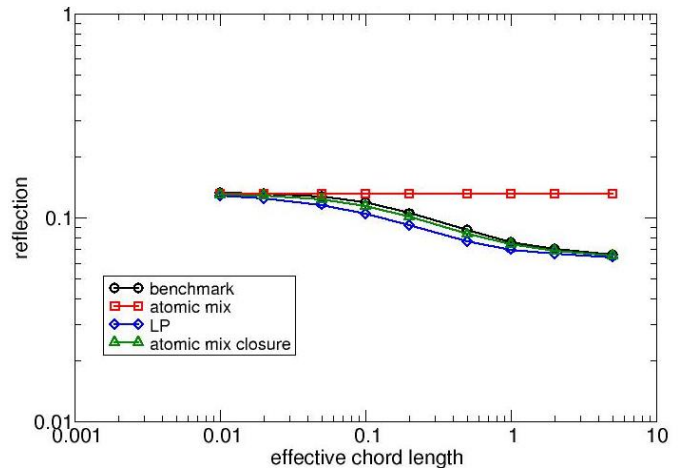


Fig. 4. Reflection results, cases 1/2, rod, $\Delta x=1$.

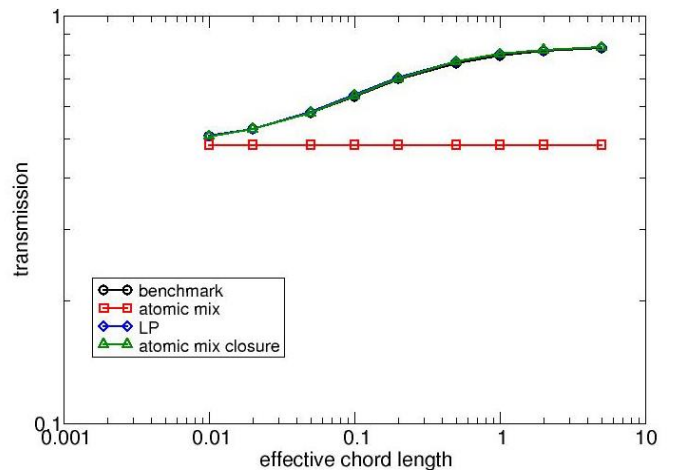


Fig. 5. Transmission results, cases 1/2, rod, $\Delta x=1$.

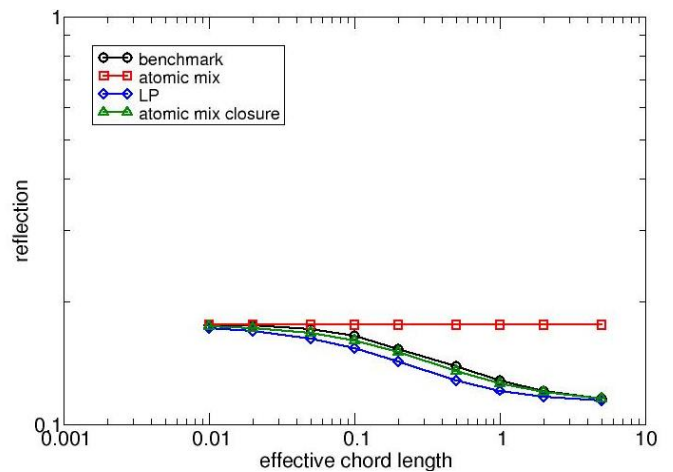


Fig. 6. Reflection results, all materials, rod, $\Delta x=1$.

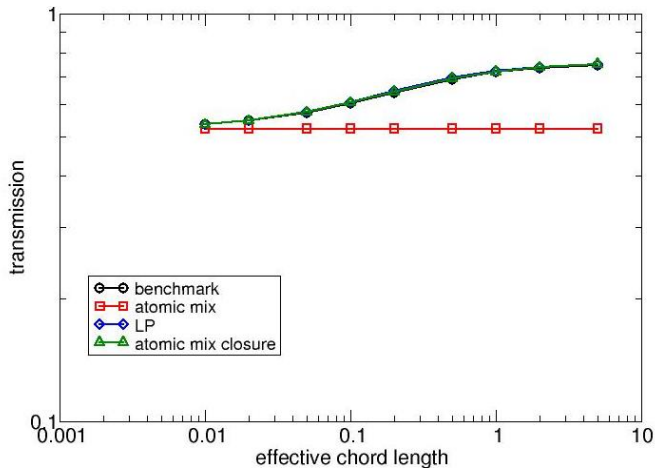


Fig. 7. Transmission results, all materials, rod, $\Delta x=1$.

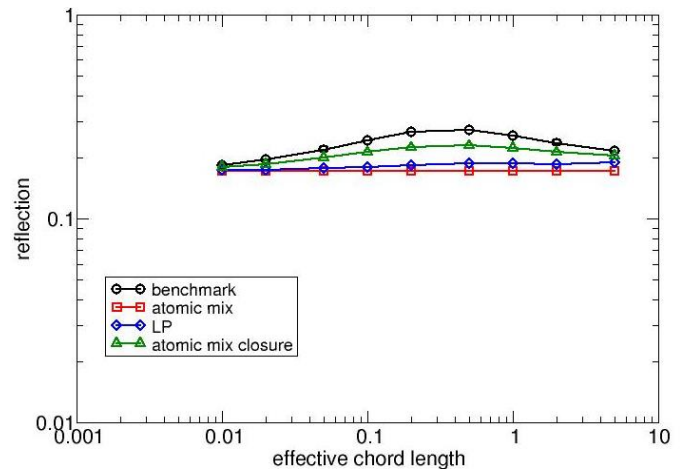


Fig. 10. Reflection results, cases 1/2, rod, $\Delta x=10$.

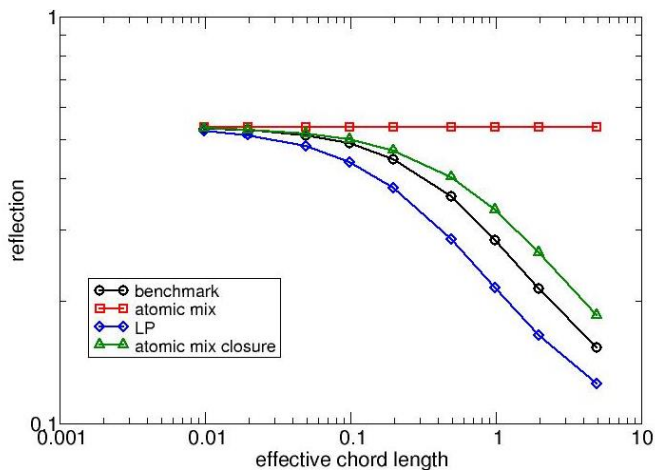


Fig. 8. Reflection results, case 1, rod, $\Delta x=10$.

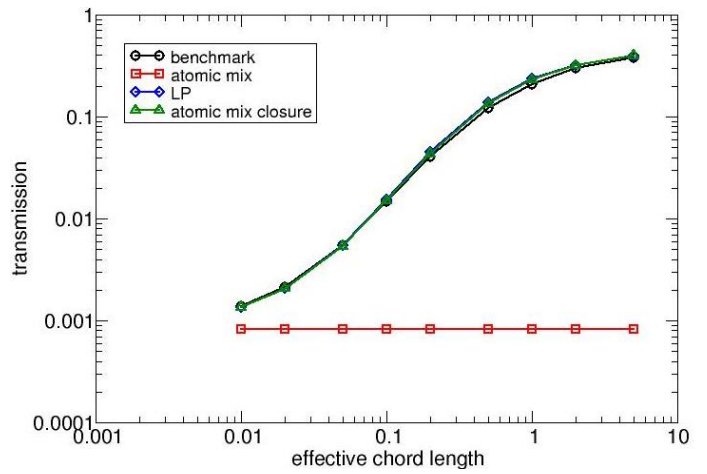


Fig. 11. Transmission results, cases 1/2, rod, $\Delta x=10$.

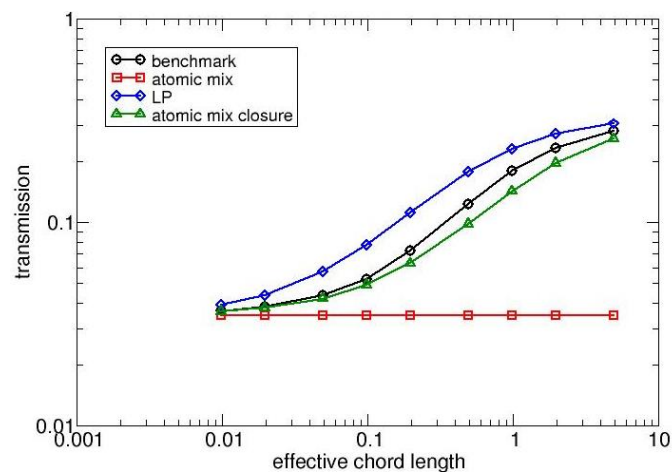


Fig. 9. Transmission results, case 1, rod, $\Delta x=10$.

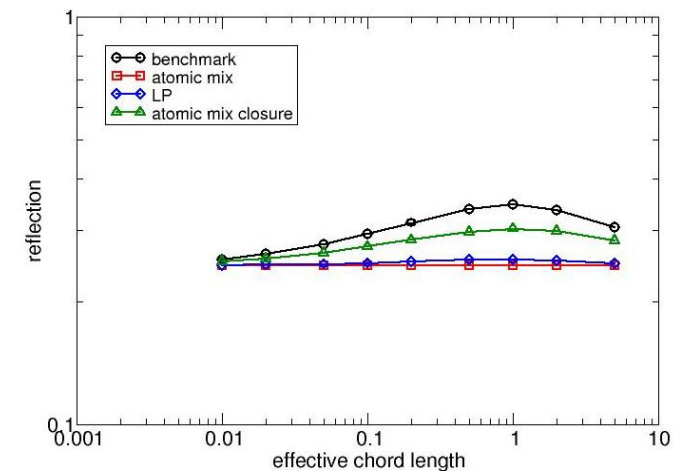


Fig. 12. Reflection results, all materials, rod, $\Delta x=10$.

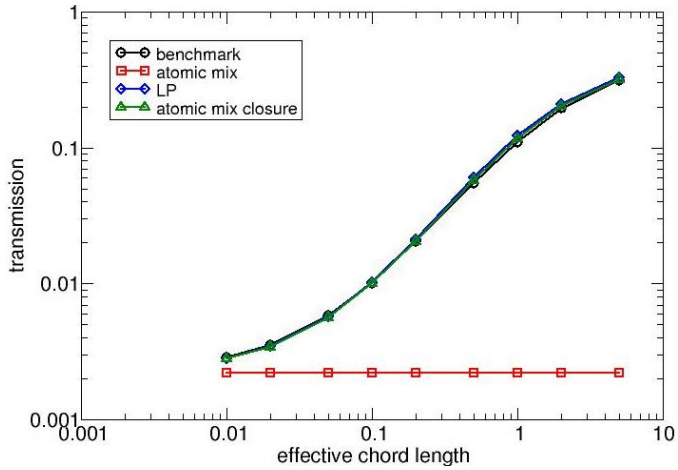


Fig. 13. Transmission results, all materials, rod, $\Delta x=10$.

We see here that the atomic mix closure is generally more accurate than LP regardless of chord length. Similar results have been observed for all of the other problems we have studied with these problem thicknesses. Only occasionally is LP slightly more accurate in the limit of very large chord lengths.

In Figures 14-19 we show results for the planar problem and $\Delta x=1$. These and other unreported results demonstrate similar behavior as the rod problems; the atomic mix closure appears to be more accurate than LP.

As noted earlier we have used the atomic mix closure matrix R generated from the center of an atomic mix realization throughout our solution of Eq. (9) rather than position-dependent closures in the above results. In general R could vary spatially. We have performed calculations that make use of spatially-dependent response matrices (not shown here), but have observed that this has little effect on the results.

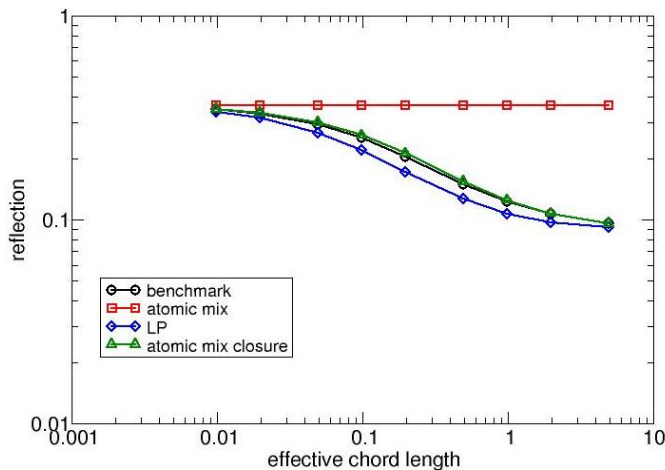


Fig. 14. Reflection results, case 1, planar, $\Delta x=1$.

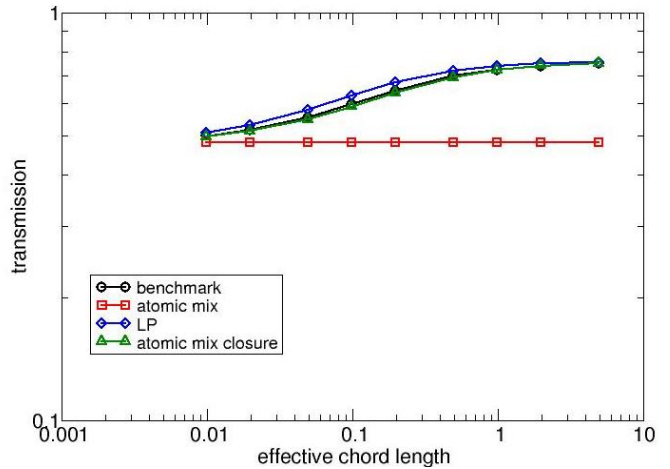


Fig. 15. Transmission results, case 1, planar, $\Delta x=1$.

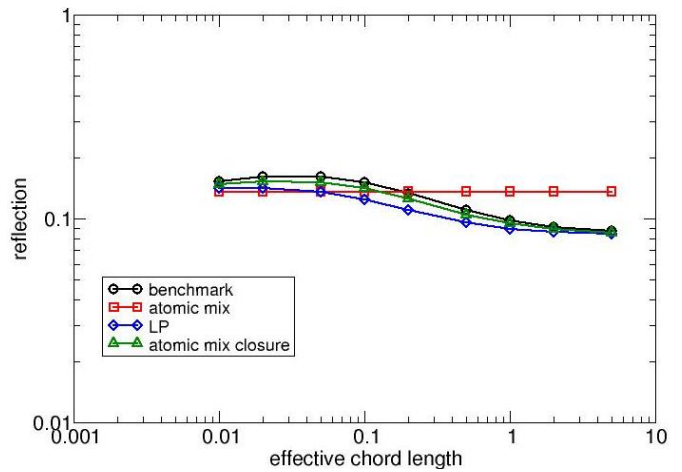


Fig. 16. Reflection results, cases 1/2, planar, $\Delta x=1$.

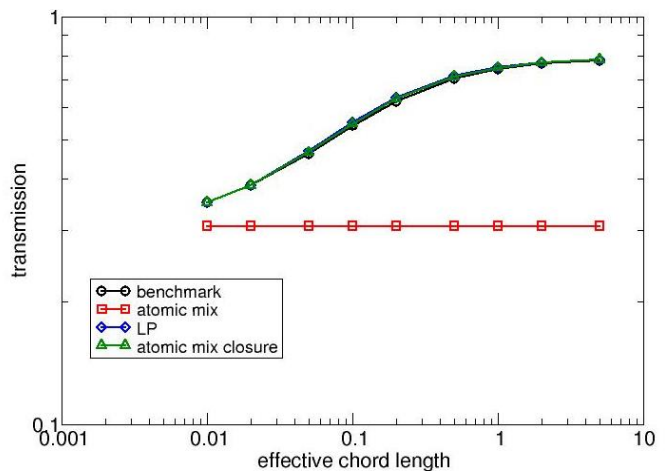


Fig. 17. Transmission results, cases 1/2, planar, $\Delta x=1$.

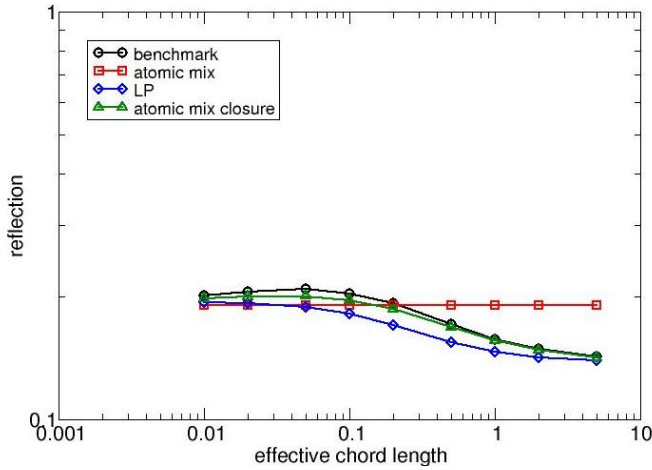


Fig. 18. Reflection results, all materials, planar, $\Delta x=1$.

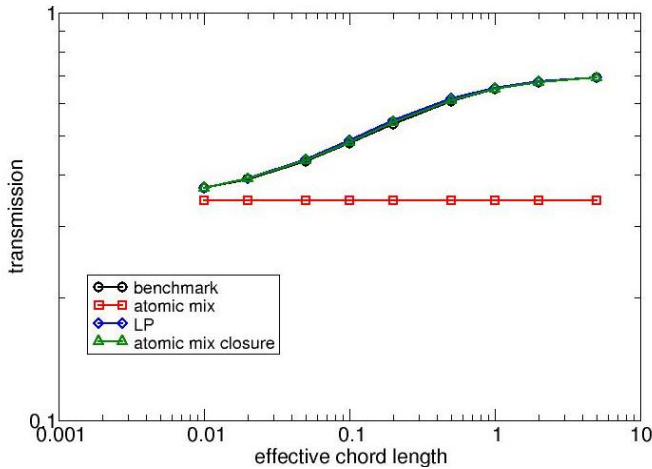


Fig. 19. Transmission results, all materials, planar, $\Delta x=1$.

We turn now to planar problems with $\Delta x=10$. These problems exhibit different behaviors than the ones reported above. In every case source iteration was observed to be unstable. Examination of R reveals that it is not diagonally-dominant in these cases. Not only will this cause source iteration to be unstable, it is not clear that a solution to the atomic mix closure equation exists. This lack of diagonal-dominance makes sense on physical grounds, since the interior fluxes in Eq. (10) will no longer be governed primarily by boundary fluxes in the same direction once there is sufficient scattering material to suppress the effects of uncollided fluxes. The notable exception will be problems with two-point quadratures, which will preserve diagonal-dominance regardless of problem thickness. This is consistent with our experience with thick rod problems reported earlier.

In order to overcome the above issue, we attempt a subgrid approach. Instead of generating R with an atomically-mixed realization of the same width as the stochastic problem, we instead use an atomically-mixed

realization with an optical thickness of unity in an attempt to guarantee diagonal-dominance while still incorporating some non-local material effects. Results generated using this subgrid approximation to R are depicted in Figures 20-25 for planar problems with $\Delta x=10$. These results appear qualitatively the same as our earlier results; the subgrid atomic-mix closure is generally more accurate than LP.

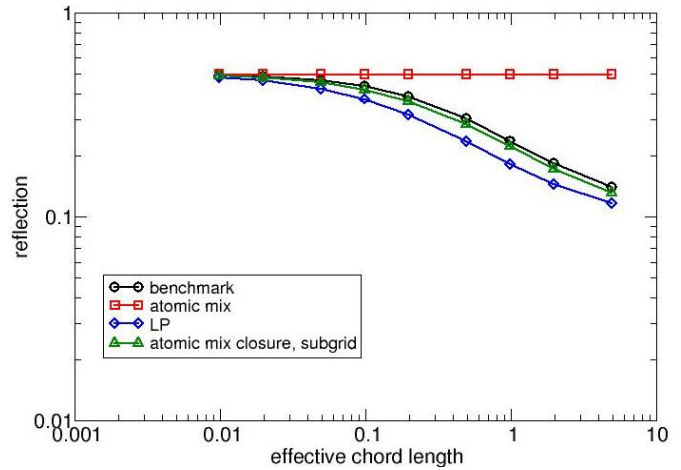


Fig. 20. Reflection results, case 1, planar, $\Delta x=10$.

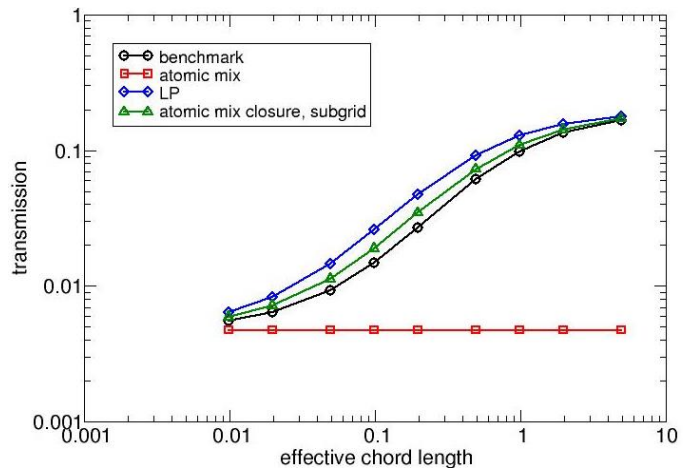


Fig. 21. Transmission results, case 1, planar, $\Delta x=10$.

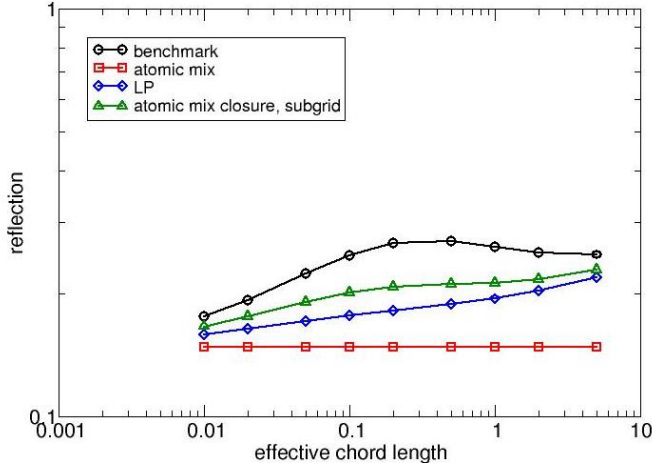


Fig. 22. Reflection results, cases 1/2, planar, $\Delta x=10$.

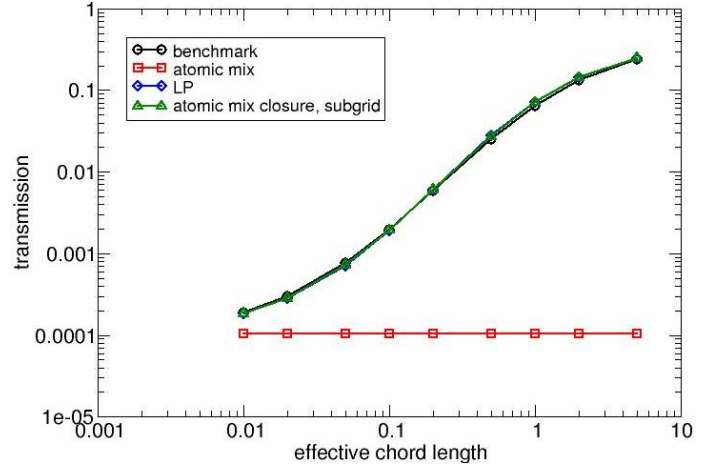


Fig. 25. Transmission results, all materials, planar, $\Delta x=10$.

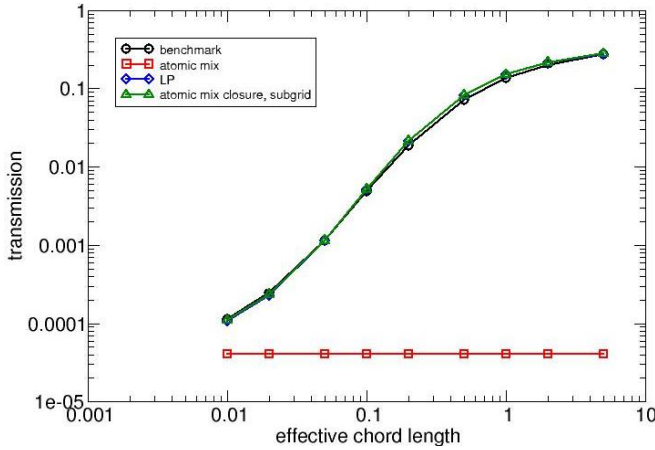


Fig. 23. Transmission results, cases 1/2, planar, $\Delta x=10$.

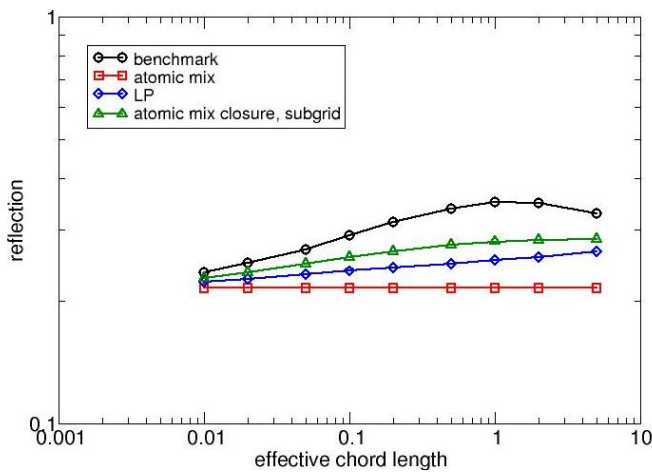


Fig. 24. Reflection results, all materials, planar, $\Delta x=10$.

IV. CONCLUSIONS

Obtaining solutions to stochastic transport problems can be quite difficult. Transport calculations on an ensemble of explicit realizations generated by Monte Carlo sampling can be prohibitively expensive. Atomic mix or LP calculations are relatively inexpensive, but they can be inaccurate. The present work illustrates an approach that is less expensive than Monte Carlo sampling yet more accurate than atomic mix or LP approximations. The atomic mix closure requires a modest number of subsidiary calculations on a single homogenized realization, which if done as a subgrid model will be less expensive than the full-geometry calculations. The same closure may be used for any chord length as long as the relative material proportions remain the same. In almost every case we have studied it is more accurate than LP.

We still need to analyze the reasons why the atomic mix closures derived for thicker problems lead to source iteration instabilities. It is not clear if the closure itself induces an ill-posed problem or if it is merely the iterative process that is problematic. We hope to examine alternative source terms to drive the subsidiary calculations. We also want to extend the work to multigroup and multidimensional problems.

NOMENCLATURE

$\Delta x_{l,am}$ = width of left atomic mix buffer region

$\Delta x_{l,r}$ = width of region(s) to left of r

$\Delta x_{r,am}$ = width of right atomic mix buffer region

$\Delta x_{r,r}$ = width of region(s) to right of r

Γ = surface between any dissimilar materials

Γ_{ij} = surface between materials i and j

λ_c = average combined chord length in stochastic material

λ_i = average chord length in material i

m_l = material at left boundary
 m_r = material at right boundary
 $m_{r,l}$ = material to left of r
 $m_{r,r}$ = material to right of r
 m^- = material at upstream boundary
 m^+ = material at downstream boundary
 m_r^- = material upstream of r
 \bar{m}_r^- = opposite of material upstream of r
 m_r^+ = material downstream of r
 μ_k = direction k of angular quadrature
 \vec{n}_i = unit outer normal on surface of material i
 Ω = direction of particle travel
 p_m = probability of material m
 $\Psi_{b,k',m}$ = boundary flux in direction k' entering material m
 $\langle \Psi_i \rangle$ = ensemble-averaged angular flux in material i
 $\langle \Psi_{s,ij} \rangle$ = ensemble-averaged angular flux at a surface leaving material i and entering material j
 q_i = internal source in material i
 Q_{ij} = geometric factor at interface between materials i and j
 r = spatial location
 R = response matrix
 R_s = surface-averaged response matrix
 R_u = unconditionally-averaged response matrix
 $\sigma_{s,i}$ = scattering cross section in material i
 $\sigma_{t,i}$ = total cross section in material i
 θ_i = net average fluxes leaving material i at interface
 V = control volume

ACKNOWLEDGMENTS

Sandia National Laboratories is a multi-mission laboratory operated by Sandia Corporation, a wholly owned subsidiary of Lockheed Martin company, for the U.S. Department of Energy's National Nuclear Security Administration under contract DE-AC04-94AL85000.

REFERENCES

1. R. SANCHEZ, "Linear Kinetic Theory in Stochastic Media," *J. Math. Phys.*, **30**, 2498 (1989).
2. O. ZUCHUAT, R. SANCHEZ, I. ZMIJAREVIC and F. MALVAGI, "Transport in Renewal Statistical Media: Benchmarking and Comparison with Models," *J. Quant. Spectrosc. Radiat. Transfer*, **51**, 689 (1994).
3. C.D. LEVERMORE, G.C. POMRANING, D.L. SANZO and J. WONG, "Linear Transport Theory in a Random Medium," *J. Math. Phys.*, **27**, 2526 (1986).
4. M.L. ADAMS, E.W. LARSEN and G.C. POMRANING, "Benchmark Results for Particle Transport in a Binary Markov Statistical Medium," *J. Quant. Spectrosc. Radiat. Transfer*, **42**, 253 (1989).
5. S.D. PAUTZ and B.C. FRANKE, "An Atomic Mix Closure for Stochastic Media Transport Problems," *Trans. American Nuclear Society*, New Orleans, Louisiana, June 12–16, 2016, American Nuclear Society (2016).
6. S.D. PAUTZ and B.C. FRANKE, "A Generalized Levermore-Pomraning Closure for Stochastic Media Transport Problems," *Proc. Joint Int. Conf. on Mathematics and Computation (M&C), Supercomputing in Nuclear Applications (SNA) and the Monte Carlo (MC) Method*, Nashville, Tennessee, April 19–23, 2015, American Nuclear Society (2015) (CD-ROM).
7. S. PAUTZ, B. BOHNHOFF, C. DRUMM and W. FAN, "Parallel Discrete Ordinates Methods in the SCEPTRE Project," *Proc. Int. Conf. on Mathematics, Computational Methods and Reactor Physics*, Saratoga Springs, New York, May 3-7, 2009, American Nuclear Society (2009) (CD-ROM).